UV photoreaction pathways of acetylacetaldehyde trapped in cryogenic matrices

P. Rousselot-Pailley, J. Mascetti, A. Pizzo, C. Aupetit, S. Sobanska, S. Coussan

UV Photoreaction Pathways of Acetylacetaldehyde Trapped in Cryogenic Matrices

P. Rousselot-Pailley,[†] J. Mascetti,[‡] A. Pizzo,[¶] C. Aupetit,[‡] S. Sobanska,[‡] and S. Coussan[*,¶]

[†]*Aix-Marseille Univ, Centrale Marseille, CNRS, iSm2 UMR 7313, Marseille, France*

[‡]*Institut des Sciences Moléculaires, Université de Bordeaux 1, CNRS UMR 5255, Talence, France.*

[¶]*Aix-Marseille Univ, CNRS, PIIM, Marseille, France*

E-mail: stephane.coussan@univ-amu.fr

Abstract

The broad band UV photochemistry kinetics of acetylacetaldehyde, the hybrid form between malonaldehyde and acetylacetone (the two other most simple molecules exhibiting an intramolecular proton transfer), trapped in four cryogenic matrices: neon, nitrogen, argon and xenon, has been followed by FTIR and UV spectroscopies. After deposition, only the two chelated forms are observed while they isomerize upon UV irradiation toward nonchelated species. From previous UV irradiation effects, we have already identified several nonchelated isomers, capable, in turn, of isomerizing and fragmenting, even fragmentation seems to be most unlikely due to cryogenic cages confinement. Based on these findings, we have attempted an approach to the reaction path of electronic relaxation. Indeed, we have demonstrated, in previous works, that in

the case of malonaldehyde, this electronic relaxation pathway proceeds through singlet states while it proceeds through triplet ones in the case of acetylacetone. We observed CO and CO_2 formations when photochemistry is almost observed among nonchelated forms, *i.e.* when parent molecule is almost totally consumed. In order to identify a triplet state transition, we have tried to observe a "heavy atom effect" by increasing the weight of the matrix gas, from Ne to Xe, and to quench T_1 state by doping the matrices with O_2. It appears that as in the case of acetylacetone, it is the nonchelated forms which fragment. It also appears that these fragmentations certainly take place in the T_1 triplet state and originate in an $\Pi^* \leftarrow n$ transition.

Introduction

Acetylacetaldehyde[1–5] (hereafter referred as AAD) is one of the most simple molecule, together with malonaldehyde[6] (hereafter referred as MA) and acetylacetone[7,8] (hereafter referred as AA), which exibits an intramolecular proton transfer between its two oxygen atoms. From our previous works, supported by selective and broad band UV and IR irradiations, together with theoretical calculations, we know that after deposition, only the chelated enol form (hereafter also referred as chelated) is present in cryogenic matrices and H is located on one O atom (Figure 1). We have also put in evidence the ability of nonchelated forms (forms producted by UV irradiations. Figure 2) to isomerize among themselves (in MA[6] and AA[7] cases, we also induced IR nonchelated $\rightleftharpoons$ nonchelated isomerizations). One of the main issue concerning this suite of simple intramolecularly H-bonded molecules, is to understand their respective electronic relaxation pathways. If in the case of MA[6] it seems that this relaxation occurs purely through singlet states, as supported by the theoretical study of *Coe et al*,[9] who put in evidence a triple conical intersection between S_0, S_1 and S_2 states, triplet states seem to be involved in that of AA.[7] Upadhyaya *et al*[10] suggested that in gas phase, upon a 266 or 248 nm irradiation, AA is initially prepared in the $^1(\pi\pi^*)$ state, then OH fragment is formed in the lowest $^3(\pi\pi^*)$ state. Upon 193 nm irradiation, AA reaches Rydberg state which crosses

over to the nearest σ^* repulsive state along C-OH bond and dissociates to give $OH^\bullet$. Phillips and co-workers[11] have carried out a comprehensive theoretical study of the photochemistry of AA. One of their main conclusion is that after having promoted $S_2 \leftarrow S_0$ transition, AA's electronic relaxation proceeds, first through a S_2/S_1 vibronic interaction, then through a conical $S_1/T_1/T_2$ intersection. They add that C-O bond breaking is the predominant phenomenon in the $^3(\pi\pi^*)$ state, and that keto-enolic tautomerization is very unlikely in gas phase. This theoretical work is strongly supported by that experimental ultrafast dynamics of Mestdagh *et al.*[12] They give a transfer time between S_2 and S_1 states of 1.4 ± 0.2 ps, after a departure from Frank-Condon region in $70\pm$ 10 ps. Therefore the question was whether or not the relaxation of AAD also involves triplet states? In cryogenic matrices two types of effects can reveal a triplet state transition: *i)* the "heavy atom effect" which would favour a transition through the triplet state by increasing the atomic or molecular weight of the matrix, which increases the spin-orbit coupling, and thus promotes Inter System Crossing (ISC) between singlet and triplet states; *ii)* the "O_2 quenching" effect which could quench triplet but also singlet states.[13–16] O_2 can also catalyse ISC of the partner molecule, keeping its triplet structure,[15,16] this phenomenon remaining minority. The complex forms between O_2 and, here, AAD, is called collision complex,[13] illustrating the necessity of a close vicinity between O_2 and AAD. This close vicinity is necessary to achieve energy transfer between AAD and O_2. The fate of this energy, once transferred from AAD to O_2, depends on the nature of the collision complex formed, with or without charge transfer. Moreover, a part of the excitation energy could remain on AAD in the form of vibrational energy, leading eventually to a further reactivity. The energy gap between the triplet level of oxygen and the singlet or triplet levels of AAD also determines the efficiency of this quenching. In our case, as we are working in the cryogenic condensed phase, the viscosity of the crystal in the quenching efficiency is not relevant. Abdel-Shafi and Worall[13] suggested that singlet state quenching by triplet state O_2 is more subtle than that of a triplet state. If O_2 singlet generation from O_2 triplet state quenching a partner triplet state as well, is weak, it could

be due to a competition between quenching and the creation of radical ions. One of the main conclusions of this work will therefore be to understand whether it is the presence of a methyl (AAD) or the coupling of the two[17] (AA), compared to MA, that causes an electronic relaxation by triplet state of the AAD.

Experimental

Matrix Experiments

Acetylacetaldehyde synthesis has already been described in details in our first publication.[1] For matrix isolation experiments carried out in Marseille, at PIIM laboratory, AAD was subjected to multiple freeze-pump-thaw cycles under primary vacuum to remove dissolved gases. AAD was then mixed with matrix gases, Ne (N50 grade, Air Liquide), Ar and N_2 (N60 grade, Air Liquide), Xe (N50 grade, Linde), in partial ratio AAD/MG (MG, matrix gas) of $\approx$ 1-6/1000 (depending on matricial gas). For the O_2 quenching experiments ratii AAD/O_2/MG varied from $\approx$ 1/1/1000 to 2/10/1000 (this last ratio has been used uniquely in Ar and N_2, *see text*). Mixtures were deposited, by pulsed deposition (Parker electromagnetic valve), onto a gold-platted copper cube cooled to 4.3 K in Ne, 20 K in Ar and N_2, and 40 K in Xe, by a closed-cycle cryogenerator PT-405 from Cryomech compagny. Cryostat and sample-carrier were protected from thermal background radiation by a chrome-platted brass shield. Controlled heating (Lakeshore Model 336) of the sample carrier was carried out with a 50 Ω resistor, while the background pressure in the vacuum chamber was kept at 10^{-7} mbar by a turbomolecular pump. Fourier transform IR (FTIR) spectra were all recorded at 4.3 K in the reflection mode using a Bruker IFS 66/S spectrometer (resolution: 0.12 cm^{-1}) equipped with a MCT detector. Broad band UV irradiation were carried out with an Oriel high-pressure mercury lamp (average power: 160 mW, no optical filter, no water filter).
For matrix isolation experiments carried out in Bordeaux, at ISM laboratory, AAD was directly mixed with Ar and N_2 in partial ratio AAD/MG of 2-4/1000 in Ar and 2/1000 in

N_2, respectively. Mixtures were deposited, at 1 mL min^{-1} rate, onto a CsI windows cooled to 15.4 K by a closed-cycle cryogenerator CTI-Cryogenics M22. IR spectra were recorded, in order to test the sample quality, in transmission mode using a Bruker Vertex 70 V at 0.5 cm^{-1} resolution. UV spectra were recorded using an UV-2600 Shimadzu spectrometer while UV irradiations were carried out with a Eurosep Instruments Hg low pressure lamp (average power: 100 mW, no optical filter, no water filter). At the difference with PIIM laboratory's experiments, in which UV beam is propagated through one CaF_2 and one KBr window over $\approx$ 60 cm, in Bordeaux, the UV lamp is located at few cm from the sample carrier, through one CaF_2 window.

All experiments were performed at least twice under exactly the same conditions.

Theoretical Calculations

UV and IR theoretical calculations have already been detailled in our past work.[1] It should be noted that Table 1 has already been published in **©Coussan et al, J. Phys. Chem. A, 2020, 124, 4916-4928, but $CCC_{OH/CO}$, TTT_{OH} $\pi^* \leftarrow \pi$ and $\pi^* \leftarrow n$ and TCT_{CO} $\pi^* \leftarrow n$ transition values were erroneous (they have been calculated with a different method: B3LYP/6-311++G(2d,2p))**. This is why we re-publish it. From UV theoretical results, three groups of UV absorptions can be conveniently discriminated as follows:

1. CCC_{CO} and CCC_{OH} with allowed transitions at 234 and 241 nm, respectively.
2. XXX_{CO} nonchelated species with allowed transitions ranging between 209 and 221 nm.
3. XXX_{OH} nonchelated species with allowed transitions ranging between 215 and 232 nm.

It is also very convenient to consider not the absolute values of the UV transitions, but rather their relative deviations, as shown in Figure 3. Following this reasoning, three groups of isomers can be redefined:

1. CCC_{OH} which serves as the origin.

2. CCC_{CO}, CTT_{OH}, CTC_{OH} and TCC_{OH} which have deviations between -7 and -14 nm.

3. The remaining isomers with deviations between -20 and -32 nm.

It is very interesting to note that the open isomers closest to CCC_{OH} are all XXX_{OH} in nature.

As detailed in the experimental results section below, we had to consider the presence of mixed AAD-water hetero-complexes, presumably dimers. We therefore performed calculations, on those hetero-complexes, in two steps: simulated annealing calculations (semi-empirical), which gives a first quick view of the semi-empirical fundamental potential surface, followed by DFT calculations on the semi-empirical minima, in order to obtain the DFT minima together with their harmonic frequency sets. This procedure has already been decribed in some of our past works.[18?] Some of those forms are shown in Figures **??** and **??** together with their relative energies with respect to the two most stable CCC_{CO}-H_2O and CCC_{OH}-H_2O forms. The main lesson of these two-step calculations is that the presence of a water molecule in the vicinity of the chelated form of AAD is sufficient to induce the opening of the pseudo-ring and consequently to observe nonchelated forms as soon as they are deposited (as discussed below in the experimental results section).
In order to identify the experimental maxima, displayed in Figures 4 and 5, we have matched the UV spectra with a deconvolution laboratory-made program.(Figure **??**).

Experimental Results and Discussion

UV Spectra

UV spectra of AAD trapped in argon and nitrogen are shown in Figures 4 and 5, respectively. What should be noted at the outset, is that it seems that there are not only chelated forms present after deposition. This fact is due to the presence of water traces in the samples as

attested by the observation of the vibrational spectra we recorded just after deposition. As can be seen from calculations on AAD-water complexes (Figures **??** and **??**), the presence of water induces the existence of nonchelated isomers. If we take into account the relative shift of these bands with respect to CCC_{OH}, they are mainly of a XXX_{OH} nature, althougth the theoretical results show that the three nonchelated forms XXX_{CO}-water are slightly more stable than those XXX_{OH}-water (Figures **??** and **??**). If we proceed by analogy by matching the nonchelated forms XXX_{CO}-water and XXX_{OH}-water, the energy differences are systematically in favour of the XXX_{CO}-water forms: CTC_{CO} is more stable than TCT_{OH} by 2.55 kcal mol^{-1}, TTC_{CO} by 3.07 kcal mol^{-1} compared to TTT_{OH} and TCT_{CO} by 1.4 kcal mol^{-1} compared to CTT_{OH}.

As reported in our first work on AAD,[1] even if these UV spectra were recorded in liquid phase and at room temperature, we should only observe two maxima separated by $\approx$ 7 nm after deposition. In argon (Figure 4), immediately after deposition, bands at 272.5 and 266.5 nm, attributed to CCC_{OH} and CCC_{CO}, respectively, can be observed, but at the same time, bands at -14.5, -24.5 and -35 nm, relative to CCC_{OH}. In nitrogen (Figure 5), one observes after deposition two bands at 269.0 and 258.5 nm, respectively assigned to CCC_{OH} and CCC_{CO}, and two others shifted by -21.5 and -32.5 nm with respect to CCC_{OH}. From the first five seconds of irradiation, the other bands in the argon and nitrogen spectra are observed at -41.5, -49 and -50.5 nm, and -43.5 and -46.5 nm, respectively. Based on the vibrational assignments made in the previous paper,[1] and by comparing the shifts in the UV absorption bands, in argon and nitrogen, with the theoretical results, we can reasonably assume that all the nonchelated isomers are formed and observed except for CCT. However, can we make a reliable electronic attribution of the UV spectra? Without selective UV irradiation, it will be hard to clearly assign all the UV bands. However, interesting information can be retrieved from the structure of these spectra. If we look closely at the theoretical results, as explained above, the nonchelated forms should present two distinct groups: one, closest to the chelated forms, comprises three XXX_{OH} forms, should present three bands on 5 nm,

and shifted to the blue between -9 and -14 nm, and a second, which presents a gap of about 6 nm with the first, should present 5 or 6 bands (at the resolution of the spectrometer, the bands of TCC_{OH}, TTT_{OH} and TTC_{OH} 1 nm apart could overlap) on 12 nm and shifted to the blue between -20 and -32 nm. Under these conditions, an approximate attribution of the UV spectra in argon and nitrogen can be as follows: the bands between -35 and -50 nm in argon can be attributed to species of the second group (furthest from XXX_{OH}), like those observed at -46.5 and -43.5 nm in nitrogen. For the other bands, if the two observed at -14.5 and -21.5 nm, in argon and nitrogen respectively, lead us to believe that they belong to the first group, as they are in proximity to the bands of the chelated forms, the situation of those at -24.5 and -32.5 nm, in argon and nitrogen, is less clear. In this respect, it is worth noting the good correlation between the band profiles recorded in these two matrices. This leads us to suggest that the latter two bands are due to the same isomer, whatever the matrix. The larger shifts in the nitrogen matrix are due to dipole-quadrupole (-OH...N_2) interactions, as already noted in our AA study.[?] This weak interaction is sufficient to shift some energy levels. It may be tempting to attribute the latter two bands also to isomers of the first group, but we cannot at this stage be completely certain.

Electronic Relaxation Pathways

As already mentioned, one of the aims of this work was to identify the electronic relaxation mechanisms of chelated and nonchelated forms, following the effects of UV broad band irradiations, by recording the vibrational spectra of the chelated and nonchelated species. We recall that MA[6] relaxes along a purely singlet path while AA[?] relaxes along a triplet path. Two phenomena can be exploited to reveal a triplet state transition: *i)* a heavy atom effect, supposed to favour an ISC (Inter System Crossing), and consequently accelerate the disappearance of the parent species or of the photo-produced, nonchelated species, which themselves photoreact; *ii)* quenching of triplet states by oxygen. For these two phenomena to take place, it is necessary that the "heavy atom" or the oxygen be in the vicinity of the

molecule whose passage through the triplet state is to be revealed. In the case of a cryogenic matrix, the rare gas atoms, from Ne to Xe, surround the doping molecules, while the oxygen must interact in a permanent way with the molecule of interest, in the injected gas phase, and this complex must survive the landing on the deposition surface. Therefore, possibly, not seeing any effect in the context of oxygen doping may come from the non-trapping in proximity of the molecule of interest and that of oxygen. During the kinetics we focus on the disappearance of the parent chelated species, and the growth of the nonchelated photoproduct species. The overall effects on the vibrational spectra of these irradiations are shown in Figures 6 and 7, and the kinetics, in the case of Ne, are shown in Figure 8.

We will not go into detail about the heavy atom effects that we have already detailed in our first work.[6] We did not observe any convincing effect of accelerated disappearance of the parent species on the kinetic constants. We renewed this work and again confirmed that we do not observe any heavy atom effect. Therefore, we focused on the oxygen quenching effects. Basically oxygen can acts in three ways : *i)* oxygen can quench singlet states; *ii)* oxygen can quench triplet states; *iii)* oxygen can catalyse intersystem crossing. Let's consider an intersystem catalysis: in this case we should have seen an effect on kinetic constants, as we should have seen a heavy atom effect. The fact is that we saw anything conlusive. If we now consider a singlet state quenching, it appears that this kind of unusual quenching is highly sensitive to diffusion.[16] As our experiments take place in cryogenic matrix at low temperature (4 K), diffusion is an extremely minor phenomenon, which we can therefore almost exclude, and with, this singlet state quenching. Let us consider the last scenario, oxygen quenches triplet states. If we first consider the vibrational spectra in Figures 6 and 7, the dashed lines at 2143 and 1820-1720 cm^{-1} represent the location of CO for the first one, while the last two delimit the area in which we should observe fragments. It is clear that without oxygen, whatever the matrix, very few fragments are observed, as well as a rather small amount of CO. One can immediately conclude that without oxygen, in matrix, fragmentation is a minority relaxation pathway. Here, already by chemical intuition, if

fragmentation is observed, considering the structure of chelated and nonchelated molecules (Figure 2), one suspects that in order to provoke a fragmentation of these structures it will be necessary to "break" the conjugation generated by the chelated structure, but also that, less important, of the nonchelated forms. To do this, a passage through a triplet state will be necessary. It can therefore be suggested that the electronic relaxation path does indeed pass through a triplet state. But who fragments? the chelated forms, as in the gas phase,[?] or the nonchelated forms? As can be seen in Figure 8, the fragmentation takes place as soon as nonchelated forms are predominant. The first conclusion is that, it is not the chelated forms which fragment, otherwise we should have seen fragmentation since the first minutes of irradiation, but uniquely nonchelated ones. Those latter forms are "easier" to fragment because their conjugated system is less delocalized than those of chelated ones. As a result we think that nonchelated forms, because of the broad band radiation of the mercury lamp, absorb in their turn UV photons which lead them to a passage by dissociated or pre-dissociated triplet state, which will be "quenched" by triplet oxygen. An additional argument in favor of this scenario is that the triplet oxygen, when it quenches the triplet state of the nonchelated forms, will be promoted into two singlet excited states $^1\Delta_g$ and $^1\Sigma_g^+$. While the former is a long-lived state, the latter is an extremely reactive state, which will either relax to the $^3\Sigma_g^-$ form, or react efficiently with radical species in its close environment. The fact that we observe not only fragments in the 1820-1720 cm^{-1} region, but also generation of CO and CO_2 (Figures 6 and 7), correlated with nonchelated forms consumption, perfectly illustrates the existence of radical oxygen in the reaction medium and thus the quenching of the triplet states of the nonchelated forms. The presence of oxygen, T_0, in its fundamental state (even if it can be much rarer S_2), thus makes it possible to reveal that indeed a fragmentation process comes into play during the electronic relaxation, not of the chelated parent forms, but of that of the photoproduced nonchelated forms. Indeed oxygen is known to be highly reactive in the presence of free radicals. Once again, the passage through a triplet state is necessary to break the conjugate system and obtain fragments. We can therefore affirm that

in the case of nonchelated species, there is indeed a passage through a triplet state. Does this mean that the relaxation of chelated forms does not pass through a triplet state? That is to say that the CCC to nC isomerisation would take place thanks to a passage through a singlet state (through a $S_2/S_1/S_0$ conical intersection), as in the case of MA[20]? There is no evidence for this, but perhaps it is due to the fact that the matrix prevents fragmentation in the case of chelated forms, even when passing through a triplet state, and that the channel largely favoured is that of isomerisation. Another experimental fact needs comment: in the Figure 6 it seems that this fragmentation occurs mainly in the Ne and Xe matrices. It is clear that fragmentation takes place in Ar and N_2, but unlike Ne and Xe, a non-negligible amount of nonchelated species remains when photostationary equilibrium is reached. This observation is accompanied by the fact that much less CO and CO_2 are generated. This fact illustrates perfectly the role played by the matrix and its influence on the relaxation processes. The fact that the observation of almost complete consumption of the nonchelated species associated with fragmentation occurs in Ne and Xe, is certainly due to the fact that Ne is the softest matrix (crystal lattice parameter: $d_{NN} = 3.16$ Å; lattice stiffness constant: $\kappa = 3.60$ $10^3 \times$ mdyn Å^{-1}) and Xe has the largest cages (crystal lattice parameter: $d_{NN} = 4.34$ Å; lattice stiffness constant: $\kappa = 10.80$ $10^3 \times$ mdyn Å^{-1}). Indeed, if the matrix allows a better diffusion of fragments because of the size of its cages or because of a low stiffness constant, it is easy to understand that after dissociation the fragments do not recombine. The argon and nitrogen matrices, which have similar characteristics (Ar: crystal lattice parameter: $d_{NN} = 3.75$ Å; lattice stiffness constant: $\kappa = 8.20$ $10^3 \times$ mdyn Å^{-1}; N_2: crystal lattice parameter: $d_{NN} = 3.99$ Å; lattice stiffness constant: $\kappa = 5.40$ $10^3 \times$ mdyn Å^{-1}), will not ease the diffusion of fragments, what will lead to their partial recombination and thus to isomerisation. This does not compromise the proposed mechanism, but illustrates that, depending on the matrices, competition between the relaxation processes does not lead to the same fragment/isomer ratii.

One last point remains to be considered: are $\Pi^* \leftarrow \Pi$ or $\Pi^* \leftarrow n$ transitions at the origin

of these matrix fragmentations, because in the case of AA, in molecular beam, it is $\Pi^* \leftarrow \Pi$ transition that is directly at the origin of the fragmentation of the chelated form.[21] To answer this question we carried out irradiations using interference filters. The effects of these irradiations on the vibrational spectra are shown in Figure 9. It is clear that whether irradiating mainly the chelated form of the CCC_{CO} type (266 nm, $\Pi^* \leftarrow \Pi$) or the nonchelated forms of the XXX_{CO} type (222 nm, $\Pi^* \leftarrow \Pi$), no fragmentation is observed; in the first case there is isomerisation of the parent form, whereas in the second case there is mainly intra-chelated forms isomerisation. The conclusion is that these fragmentations are therefore due to transitions of the $\Pi^* \leftarrow n$ type, in the case of the nonchelated forms. One of these bands is observed at 443 nm in Ar (Figure **??**).

Conclusion

In this work, we investigated the broadband UV photochemistry of the hybrid form of malonaldehyde and acetylacetone, acetylacetaldehyde (Figure 2), trapped in four different matrices, Ne, Ar, N_2 and Xe. This species presents two distinct forms at 4 K, whether for the chelated form, which is the only one present after deposition, or the nonchelated, photoproduced forms, because the proton is localised. One of the main questions we wanted to answer was whether the electronic relaxation path of acetylacetaldehyde was a triplet path, like acetylacetone, or singlet like malonaldehyde. And consequently to know if this difference in behaviour was due to the coupling between the two methyls.[?] To detect a triplet state, two effects were explored, heavy atom effects and quenching of triplet states by oxygen. These two types of experiments did not give salient results, notably on the value of the kinetic constants, but on the other hand, oxygen doping revealed a transition to a triplet state in the case of UV photochemistry of nonchelated species. In the presence of oxygen, which in its T_0 form is a particularly reactive with free radicals, fragmentation of the nonchelated species was observed, with subtle differences in the fragment to isomer ratio depending on the matrix.

This fragmentation process is particularly visible in the Ne and Xe matrices, which are respectively the softest (Ne), and the most spacious (Xe), allowing for non-recombinatorial diffusion of these fragments. The last two of the conclusions reached are that, unlike in the gas phase, it is $\Pi^* \leftarrow n$ type transitions that are at the origin of these fragmentations, and it is therefore not the coupling between the two methyls (in AA case compared to MA) that causes this electronic relaxation through the triplet state. Consequently, the end of the work on this trilogy can be summarised as follows (Figure 10): malonaldehyde exhibits electronic relaxation through singlet states, whereas acetylacetone and acetylacetaldehyde relax through triplet states. In the gas phase, acetylacetone fragments by excitation of $\Pi^* \leftarrow \Pi$ transitions of the chelated form, while in cryogenic matrix, the latter molecule as well as acetylacetaldehyde fragment by excitation of $\Pi^* \leftarrow n$ transitions of the nonchelated forms.

Supplementary Material

This section contains two figures, labelled S1 and S2, diplaying the four calculated lowest energy AAD-water hetero dimers, one figure, labelled S3, displaying an example of UV spectrum devonvolution, and a last figure, labelled S4, displaying the full UV spectrum of AAD trapped in argon matrix.

Acknowledgements

The authors would like to thank Mrs Frédérique Berger, glassblower, and Mr Grégory Giacometti and Mr Alexandre Poyé, for their technical assistance. It was Alexandre Poyé who developed the UV spectra band deconvolution programme.

Table 1: Theoretical UV transitions calculated for the two first excited electronic states of each AAD isomers at the ωB97XD/6-311++G(2d,2p) level of theory (allowed transitions are written in bold characters). *This Table has already been published in* ***©Coussan et al, J. Phys. Chem. A, 2020, 124, 4916-4928, but*** $CCC_{OH/CO}$, TTT_{OH} $\pi^* \leftarrow \pi$ ***and*** $\pi^* \leftarrow n$ ***and*** TCT_{CO} $\pi^* \leftarrow n$ ***transition values were erroneous (they have been calculated with a different method: B3LYP/6-311++G[2d,2p]).*** *Erroneous values are given in parenthesis for information.*

Isomers	Transition	Wavelength (eV)	Wavelength (nm)	Oscillator strengths
CCC_{CO}	$S_1 \leftarrow S_0/\pi^* \leftarrow n$	4.3377	285*(300)*	0.0007*(0.0006)*
	$S_2 \leftarrow S_0/\pi^* \leftarrow \pi$	5.3017	**234***(241)*	0.2510*(0.2353)*
CCC_{OH}	$S_1 \leftarrow S_0/\pi^* \leftarrow n$	4.2269	283*(308)*	0.0010*(0.0009)*
	$S_2 \leftarrow S_0/\pi^* \leftarrow \pi$	5.1339	**241***(248)*	0.2866*(0.2717)*
CCT_{CO}	$S_1 \leftarrow S_0/\pi^* \leftarrow n$	3.8909	319	0.0003
	$S_2 \leftarrow S_0/\pi^* \leftarrow \pi$	5.6969	**218**	0.3390
CCT_{OH}	$S_1 \leftarrow S_0/\pi^* \leftarrow n$	3.7335	332	0.0006
	$S_2 \leftarrow S_0/\pi^* \leftarrow \pi$	5.4595	**227**	0.3829
CTC_{CO}	$S_1 \leftarrow S_0/\pi^* \leftarrow n$	4.1344	300	0.0001
	$S_2 \leftarrow S_0/\pi^* \leftarrow \pi$	5.6561	**219**	0.3315
CTC_{OH}	$S_1 \leftarrow S_0/\pi^* \leftarrow n$	3.9257	316	0.0006
	$S_2 \leftarrow S_0/\pi^* \leftarrow \pi$	5.3902	**230**	0.3528
CTT_{CO}	$S_1 \leftarrow S_0/\pi^* \leftarrow n$	4.1178	301	0.0001
	$S_2 \leftarrow S_0/\pi^* \leftarrow \pi$	5.5999	**221**	0.3293
CTT_{OH}	$S_1 \leftarrow S_0/\pi^* \leftarrow n$	3.9075	317	0.0005
	$S_2 \leftarrow S_0/\pi^* \leftarrow \pi$	5.3392	**232**	0.3551
TCC_{CO}	$S_1 \leftarrow S_0/\pi^* \leftarrow n$	4.1554	298	0.0002
	$S_2 \leftarrow S_0/\pi^* \leftarrow \pi$	5.7360	**216**	0.3489
TCC_{OH}	$S_1 \leftarrow S_0/\pi^* \leftarrow n$	4.0061	309	0.0005
	$S_2 \leftarrow S_0/\pi^* \leftarrow \pi$	5.4518	**227**	0.4013
TCT_{CO}	$S_1 \leftarrow S_0/\pi^* \leftarrow n$	4.0700	305*(310)*	0.0002*(0.0002)*
	$S_2 \leftarrow S_0/\pi^* \leftarrow \pi$	5.8784	**211**	0.3756
TCT_{OH}	$S_1 \leftarrow S_0/\pi^* \leftarrow n$	3.8900	319	0.0004
	$S_2 \leftarrow S_0/\pi^* \leftarrow \pi$	5.6012	**221**	0.4589
TTC_{CO}	$S_1 \leftarrow S_0/\pi^* \leftarrow n$	4.1763	297	0.0002
	$S_2 \leftarrow S_0/\pi^* \leftarrow \pi$	5.9195	**209**	0.4142
TTC_{OH}	$S_1 \leftarrow S_0/\pi^* \leftarrow n$	4.0964	303	0.0003
	$S_2 \leftarrow S_0/\pi^* \leftarrow \pi$	5.7732	**215**	0.4823
TTT_{CO}	$S_1 \leftarrow S_0/\pi^* \leftarrow n$	4.1365	300	0.0002
	$S_2 \leftarrow S_0/\pi^* \leftarrow \pi$	5.8749	**211**	0.4191
TTT_{OH}	$S_1 \leftarrow S_0/\pi^* \leftarrow n$	4.0577	305*(326)*	0.0003*(0.0002)*
	$S_2 \leftarrow S_0/\pi^* \leftarrow \pi$	5.7295	**216***(231)*	0.4848*(0.1514)*

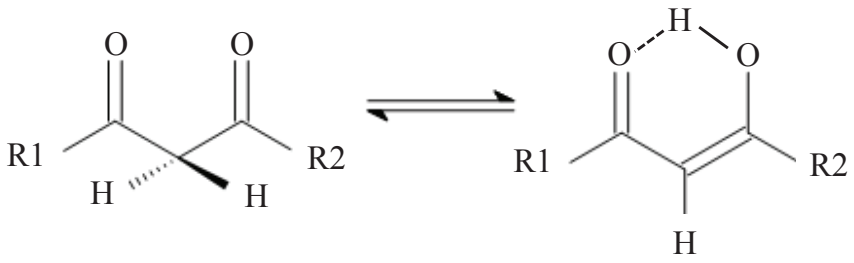

Keto Enol

R1 : H or CH_3
R2 : H or CH_3

Figure 1: Keto-Enol equilibrium of malonaldehyde, acetylacetone and acetylacetaldehyde ($R1 = H, R2 = CH_3$, and *vice-versa*). ***©Coussan et al, J. Phys. Chem. A, 2020, 124, 4916-1928***

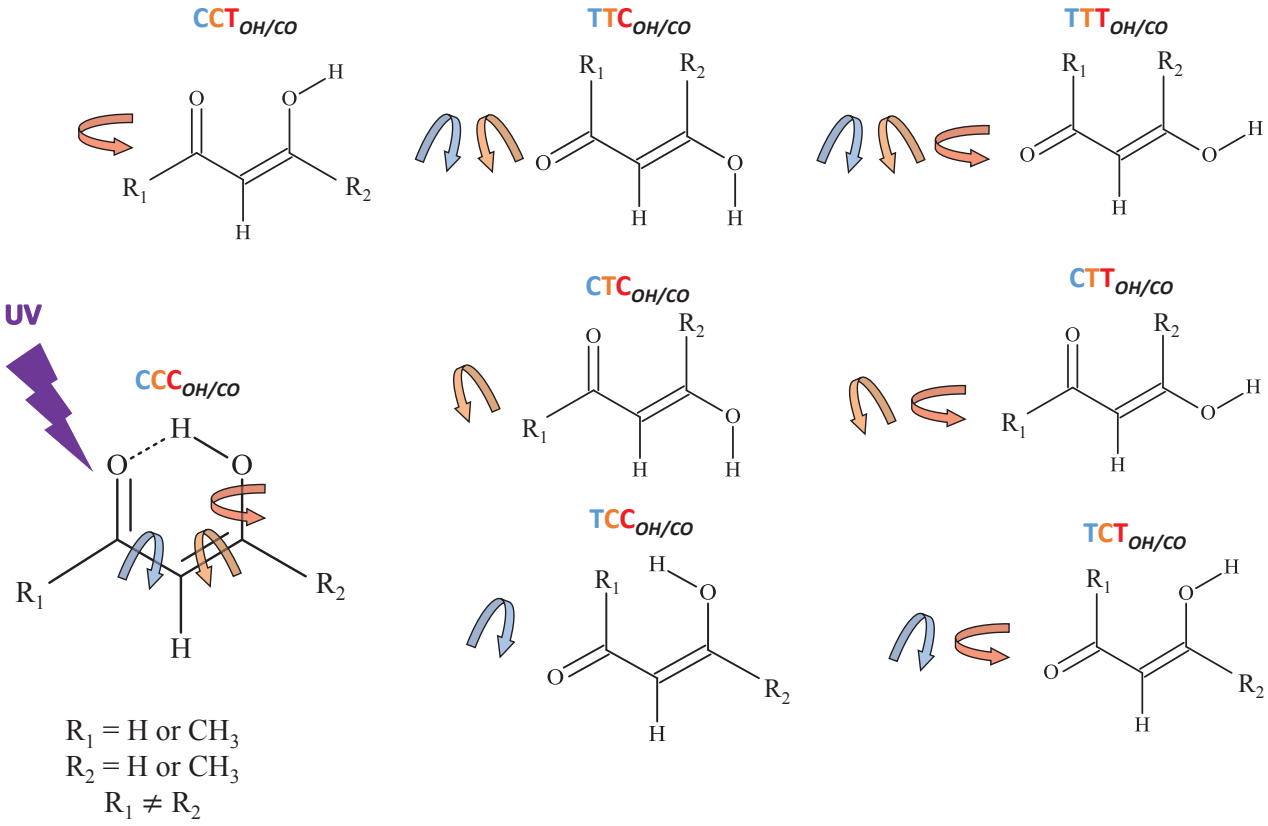

Figure 2: Picture of all AAD isomers. Nonchelated forms are obtained by UV irradiation of CCC, only form present after deposition. C and T stand for *Cis* and *Trans* characters relative to C-C, C=C and C-O bonds. OH and CO underscripts stand for the "side" methyl group is attached, or C=O or O-H one. For relative energies obtained at the B3LYP/6-311G++(2d,2p) level of theory, see ***©Coussan et al, J. Phys. Chem. A, 2020, 124, 4916-1928***.

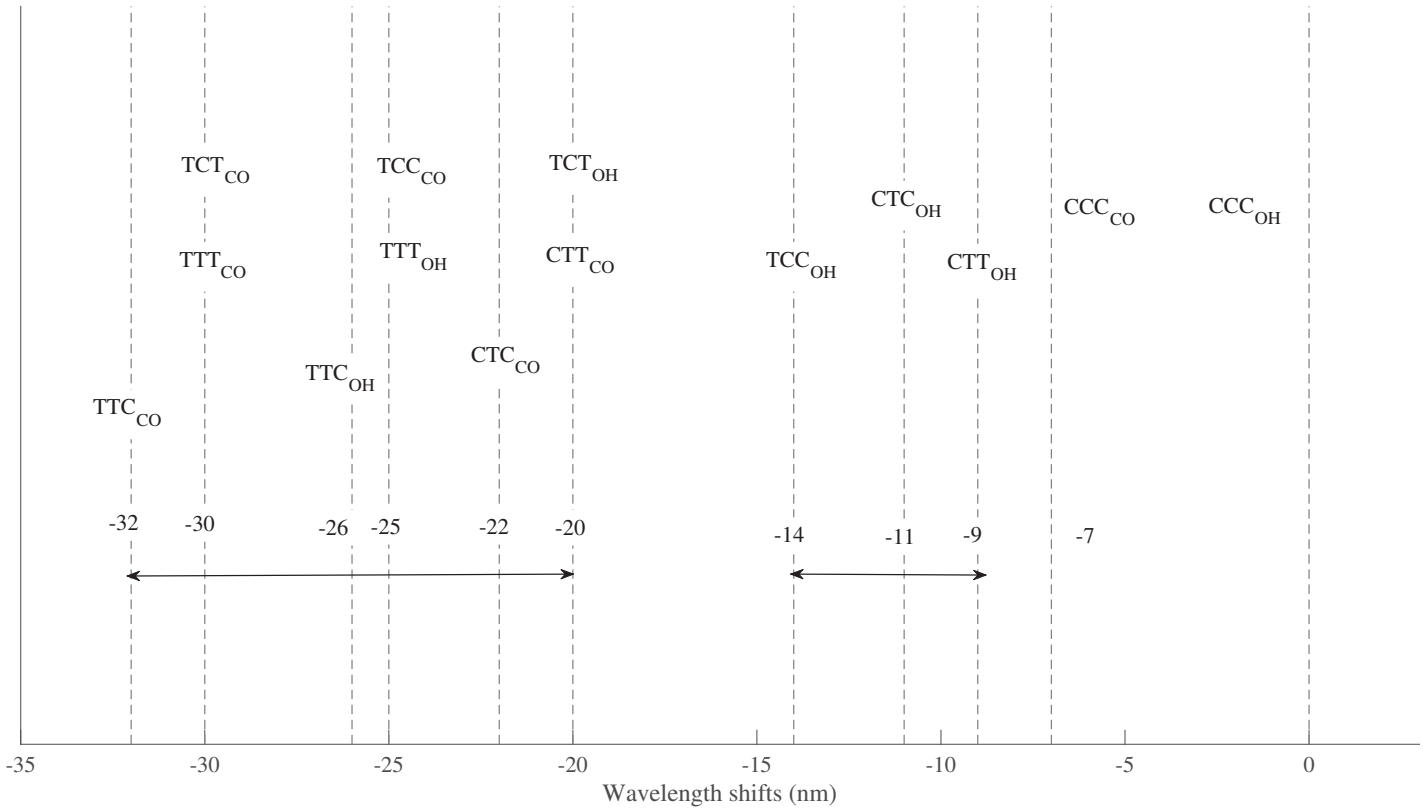

Figure 3: Theoretical UV absorption shifts with respect to CCC_{OH}. $CCT_{OH/CO}$ are not represented because they are not observed.[1]

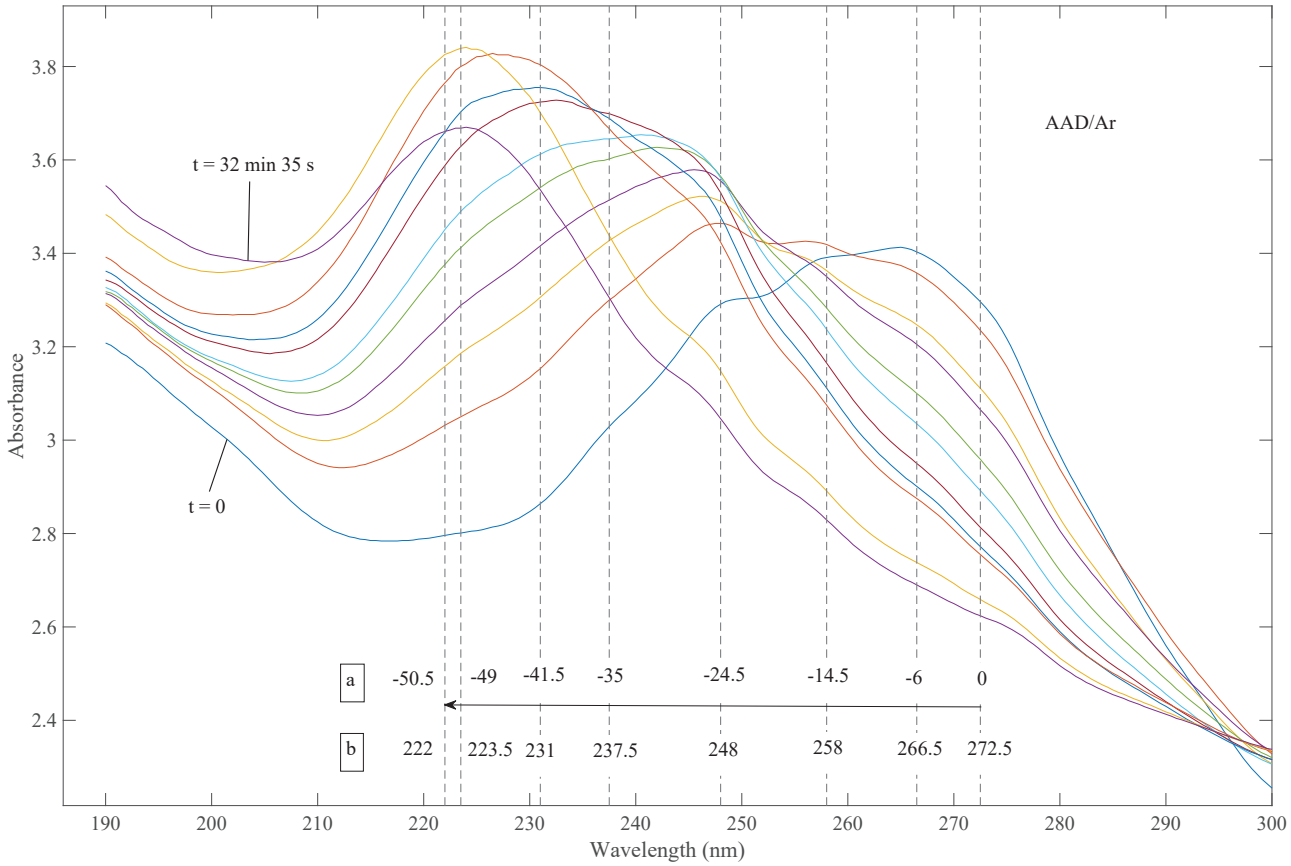

Figure 4: Evolution of the UV spectra of AAD trapped in argon matrix (AAD/Ar = 2/1000) under broadband UV irradiation (average power 100 W, no water filter, the beam was not focused). The original spectrum is noted t=0, the final spectrum t=32min35s. The irradiation times are: 5s, 10s, 15s, 25s, 35s, 65s, 2min5s, 3min5s, 13min5s, 32min35s. The relative shifts (a) are calculated with respect to the band at 272.5 nm. The wavelength (b) values have been given by deconvolution fits presented in Figure S1.

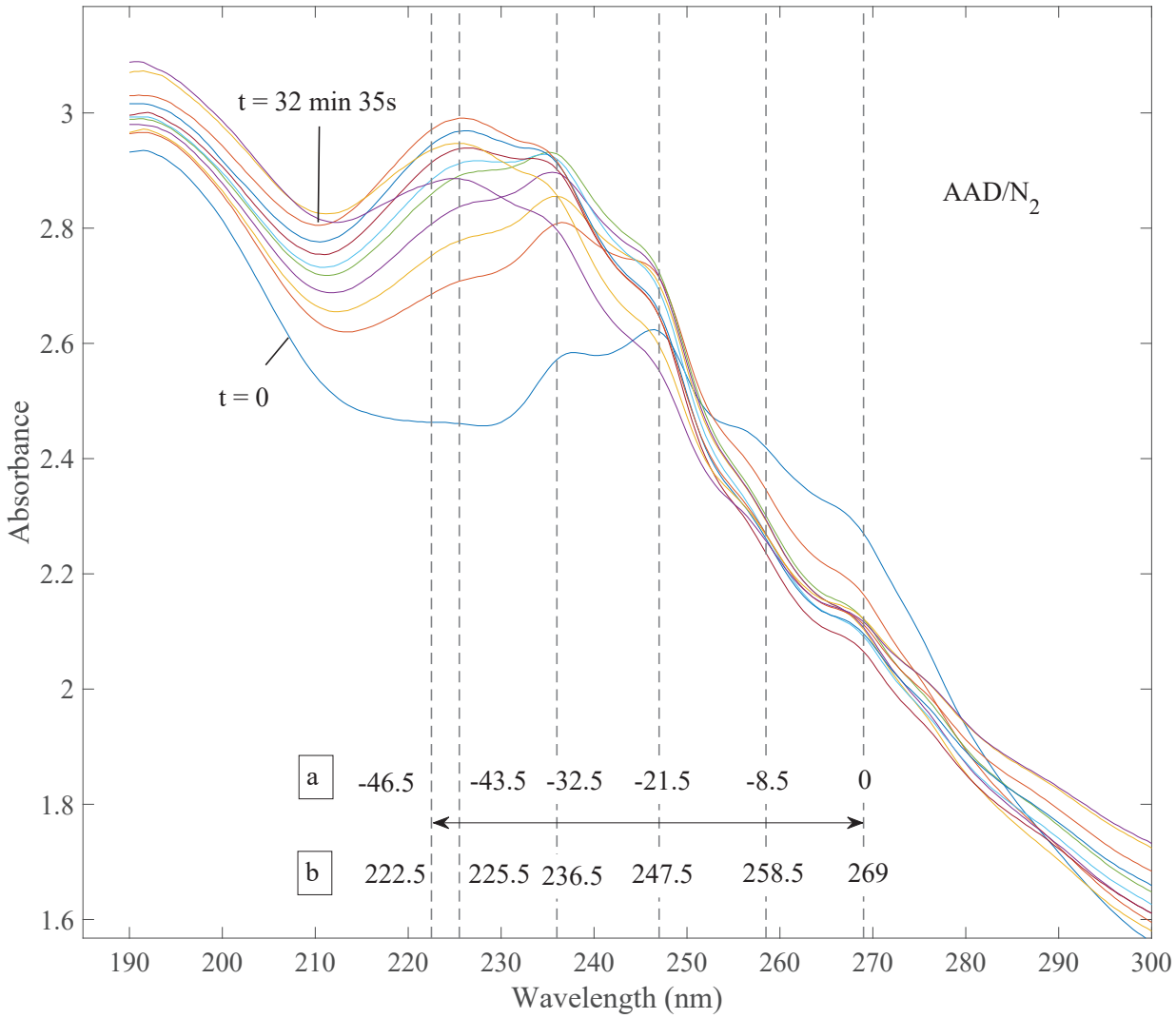

Figure 5: Evolution of the UV spectra of AAD trapped in nitrogen matrix (AAD/N_2 = 2/1000) under broadband UV irradiation (average power 100 W, no water filter, the beam was not focused). The original spectrum is noted t=0, the final spectrum t=32min35s. The irradiation times are: 5s, 10s, 15s, 25s, 35s, 65s, 2min5s, 3min5s, 13min5s, 32min35s. The relative shifts (a) are calculated with respect to the band at 272.5 nm. The wavelength (b) values have been given by deconvolution fits presented in Figure S1.

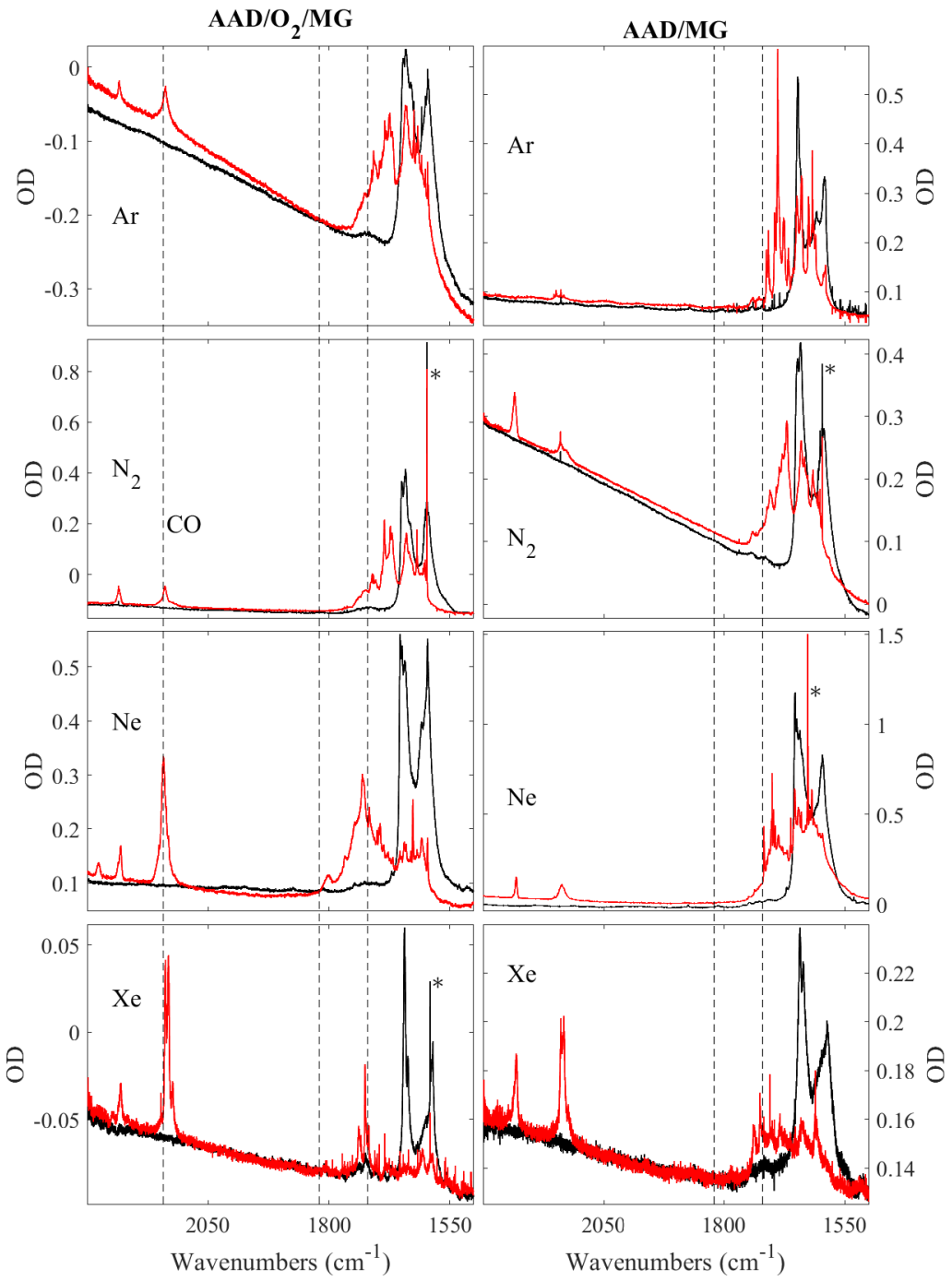

Figure 6: Effects of O_2 doping observed in the four matrices in $\nu_{C=C/C=O}$ region. Black spectra: spectra after deposition; red spectra: spectra after UV broad band irradiation. Average UV lamp power: 160 W (no beam focussing, no water filter), excepted for AAD/Ar matrice for which a 300 W power has been used. Dashed lines are centered at 2143 (CO), 1820 and 1720 cm^{-1}. The last two delimit the region in which the AAD fragments are to be observed. MG: Matrical gas. Ar: AAD/Ar = 5/1000, irradiation time: 500 min; AAD/O_2/Ar = 2/10/1000, irradiation time: 509 min. N_2: AAD/N_2 $\approx$ 2/1000, irradiation time: 509 min; AAD/O_2/N_2 = 2/10/1000, irradiation time: 509 min. Ne: AAD/Ne = 3/1000, irradiation time: 509 min; AAD/O_2/Ne = 2/2/1000, irradiation time: 629 min. Xe: AAD/Xe = 1/1000, irradiation time: 509 min; AAD/O_2/Xe = 3/3/1000, irradiation time: 469 min.$*$ traces of water.

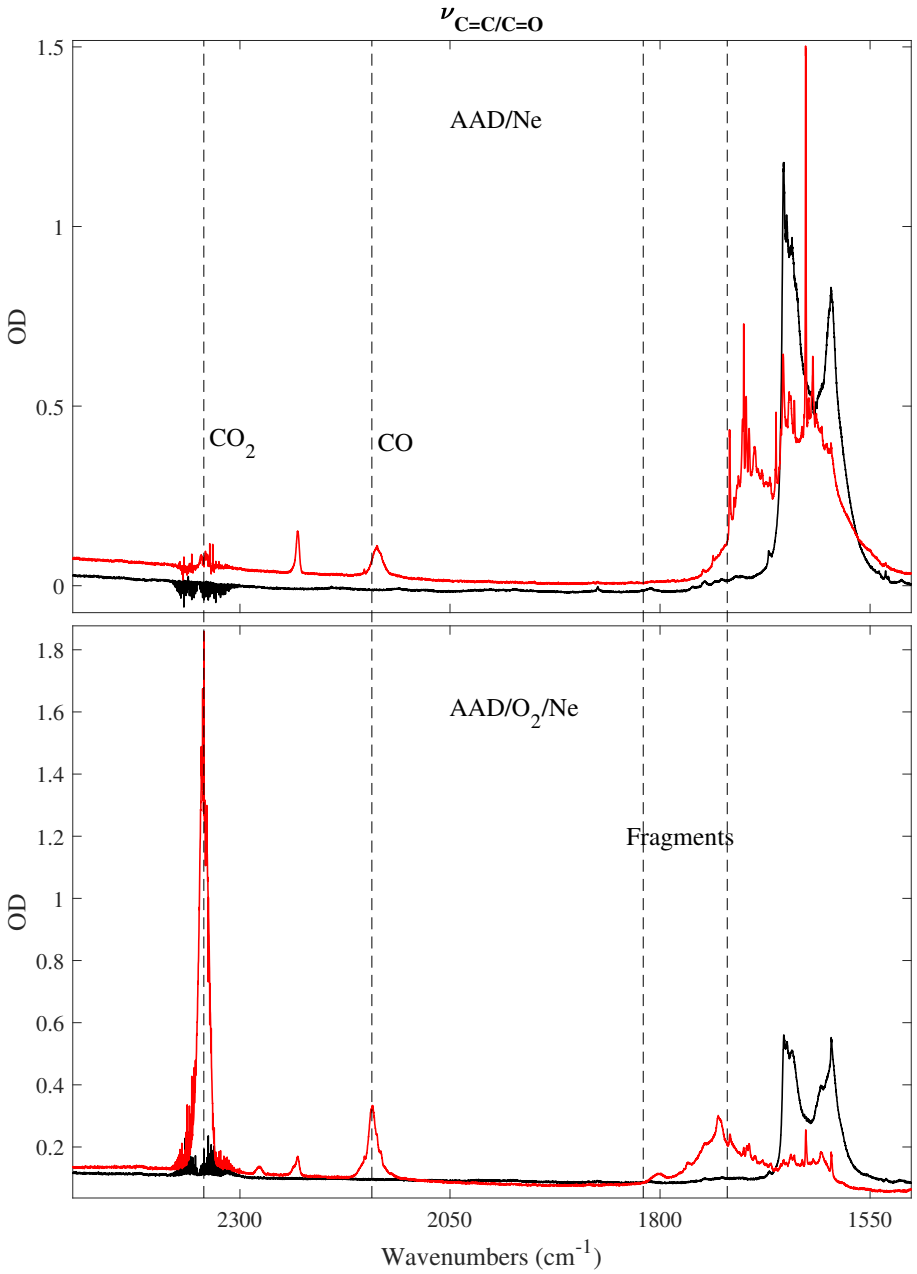

Figure 7: Effects of O_2 doping observed in Ne matrice in $\nu_{C=C/C=O}$ region. Black spectra: spectra after deposition; red spectra: spectra after UV broad band irradiation. Average UV lamp power: 160 W (no beam focussing, no water filter). Dashed lines are centered at 2343 (CO_2), 2143 (CO), 1820 and 1720 cm^{-1}. The last two delimit the region in which the AAD fragments are to be observed. AAD/Ne = 3/1000, irradiation time: 509 min; AAD/O_2/Ne = 2/2/1000, irradiation time: 629 min.

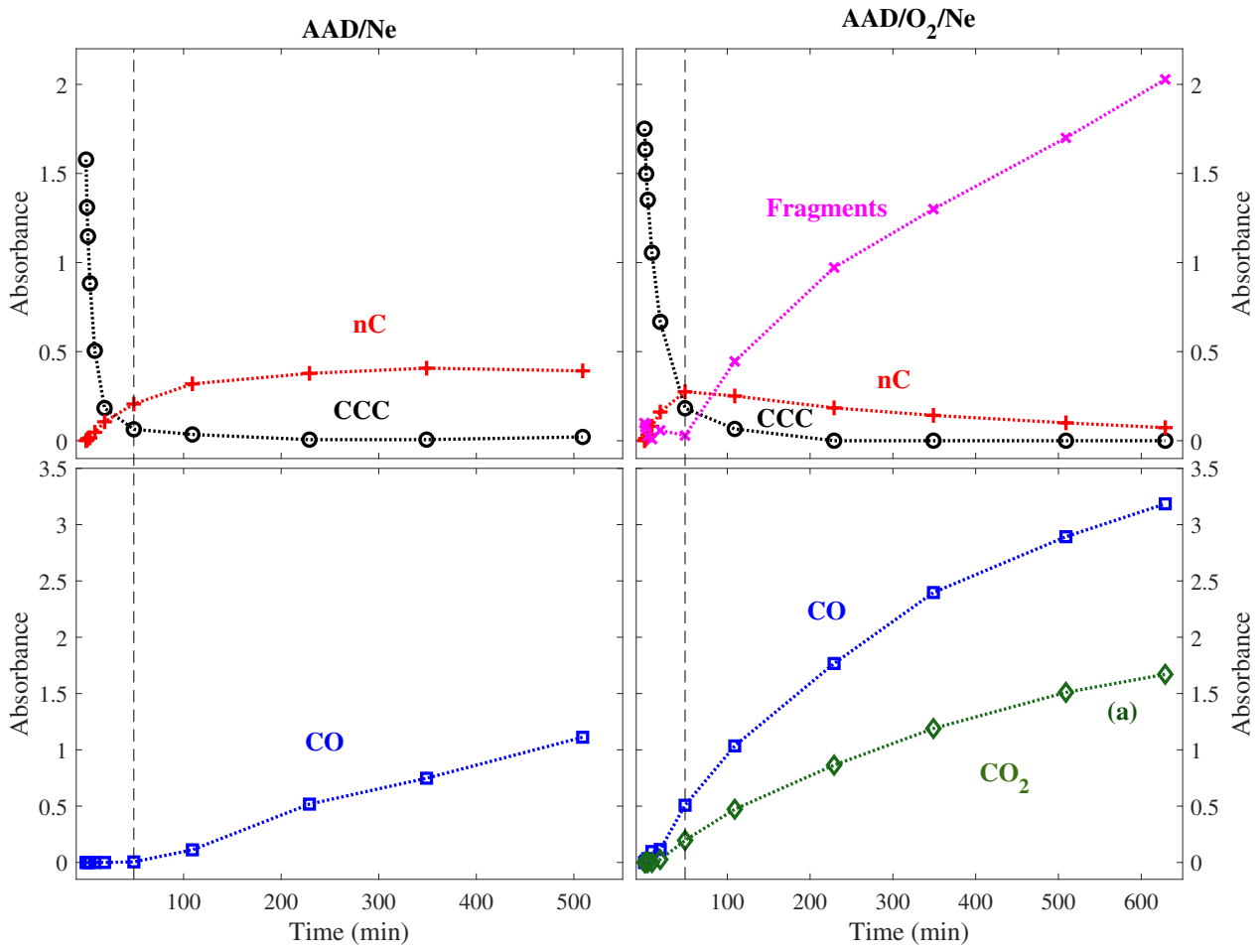

Figure 8: Kinetics in Ne with (right column) and without oxygen (left column). These kinetics were recorded at 4K. These kinetics were recorded without the use of a water filter and without focusing the beam, at an average power of 160 W. CCC: chelated forms; nC: non-chelated forms $CTT_{OH}/CTC_{OH}/CTC_{CO}$.[1] (a): CO_2 values have been divided by 10. Integration intervals for CCC: 1476-1452 cm^{-1}; for nC: 1718.6-1712.9 cm^{-1}; for CO: 2166-2118 cm^{-1}; for CO_2: 2358-2362 cm^{-1}; for fragments: 1780-1720 cm^{-1}. Dashed line is located at 49 min. Values have not been normalized.

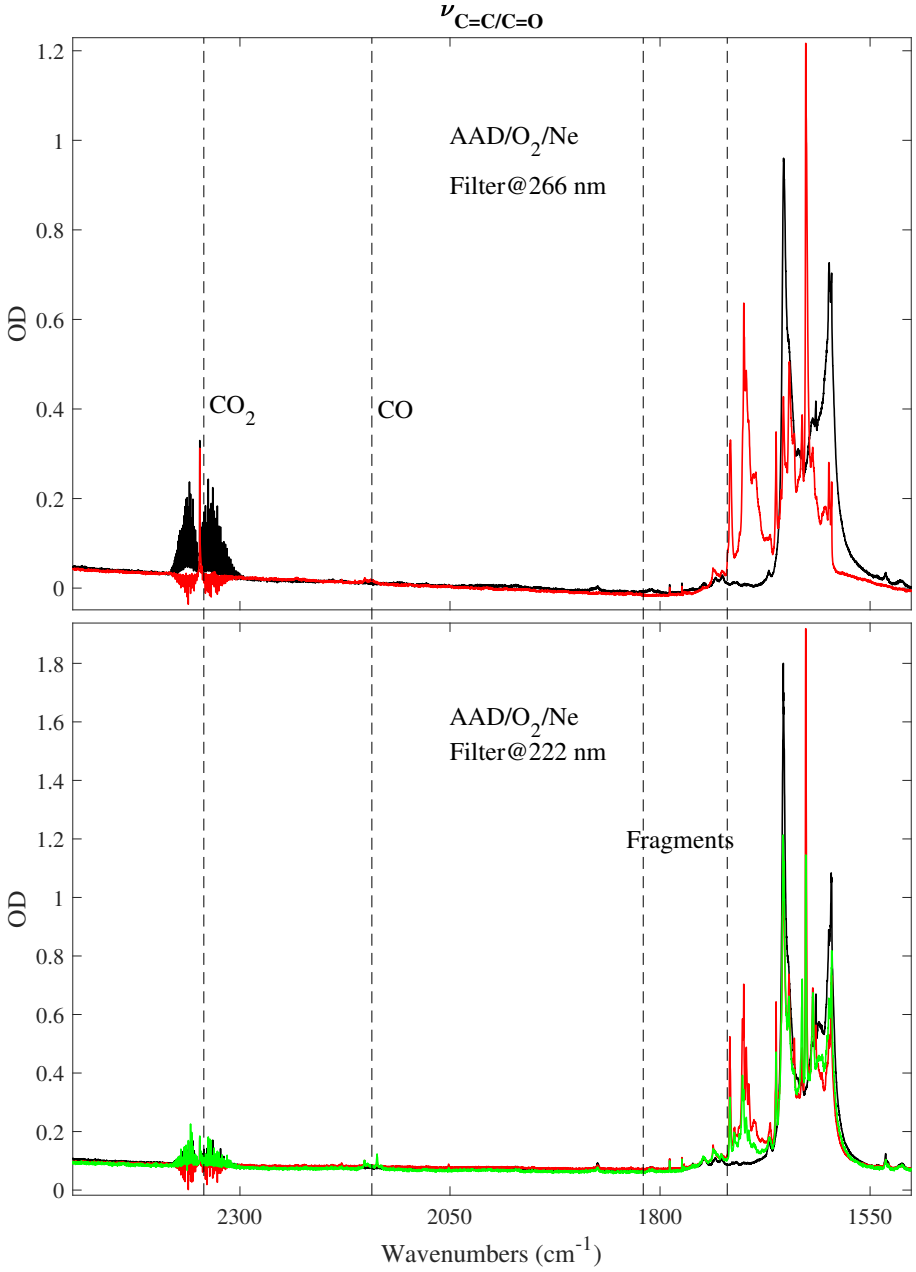

Figure 9: Effects of interferential filters on O_2 doped Ne matrice in $\nu_{C=C/C=O}$ region. Average UV lamp power: 160 W (no beam focussing, no water filter). Dashed lines are centered at 2343 (CO_2), 2143 (CO), 1820 and 1720 cm^{-1}. The last two delimit the region in which the AAD fragments are to be observed. Bottom spectra: AAD/O_2/Ne = 1/1/1000. Black spectra: spectra after deposition; green spectra: after 4 min irradiation without filter, to get nonchelated forms, red spectra: spectra after 505 min UV broad band irradiation using a 50% transmission filter centered at 222 nm. Top spectra: AAD/O_2/Ne = 1/1/1000. Black spectra: spectra after deposition; red spectra: spectra after 509 min UV broad band irradiation using a 50% transmission filter centered at 266 nm.

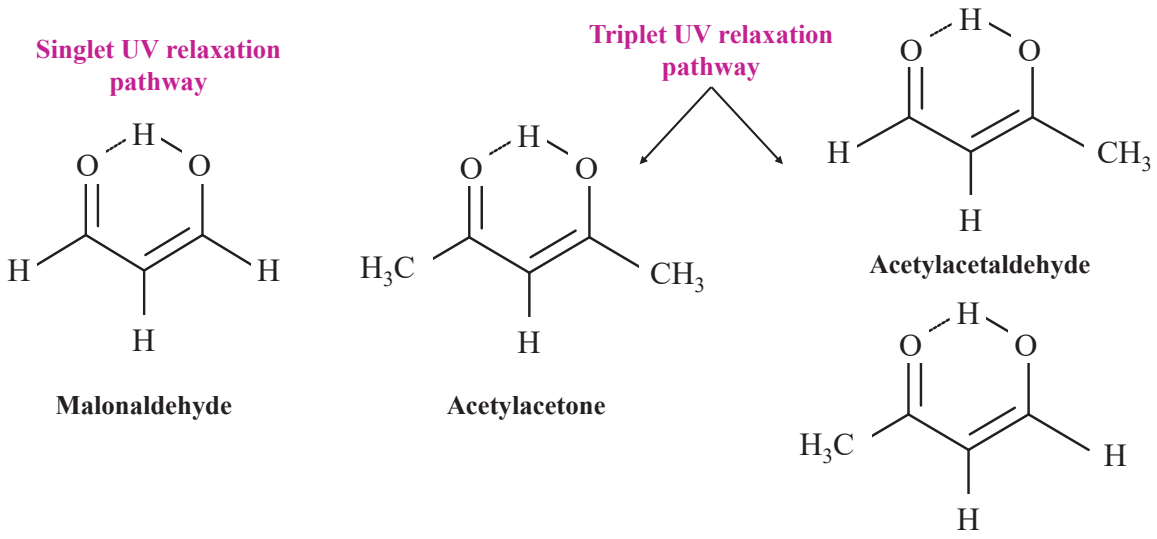

Figure 10: UV relaxation pathways: history of a trilogy.

References

(1) Rousselot-Pailley, P.; Sobanska, S.; Ferré, N.; Coussan, S. UV Photochemistry of Acetylacetaldehyde Trapped in Cryogenic Matrices. *J. Phys. Chem. A*, **2020**, *124*, 4916-4928.

(2) Chiavassa, T.; Verlaque, P.; Pizzala, L.; Roubin, P. Vibrational Studies of Methyl Derivatives of Malonaldehyde: Determination of a Reliable Force Field for β-dicarbonyl Compounds. *Spectrochimica Acta A*, **1994**, *50A*, 343-351.

(3) Bothner-By, A. A.; Harris, R. K. Conformational Preferences in Malondialdehyde and Acetylacetaldehyde Enols Investigated by Nuclear Magnetic Resonance. *J. Org. Chem.*, **1965**, *30*, 254-257.

(4) George, W. O.; Mansell, V. G. Nuclear Magnetic Resonance Spectra of Acetylacetaldehyde and Malondialdehyde. *J. Chem. Soc. B*, **1968**, , 132-134.

(5) Nowroozi, A.; Jalbout, A. F.; Roohi, H.; Khalilinia, E.; Sadeghi, M.; De Leon, A.; Raissi, H. Hydrogen Bonding in Acetylacetaldehyde: Theoretical Insights from the Theory of Atoms in Molecules. *Int. Quantum Chem.*, **2009**, *109*, 1505-1514.

(6) Trivella, A.; Wassermann, T. N.; Manca Tanner, C; Lüttschwager, N. O. B.; Coussan, S. UV and IR Photochemistries of Malonaldehyde Trapped in Cryogenic Matrices. *J. Phys. Chem. A*, **2018**, *122*, 2376-2393.

(7) Trivella, A.; Wassermann, T. N.; Mestdagh, J.M.; Manca Tanner, C; Marinelli, F; Roubin, P.; Coussan, S. New Insights into the Photodynamics of Acetylacetone: Isomerization and Fragmentation in Low-Temperatures Matrixes. *PCCP*, **2010**, *12*, 8300-8312.

(8) Trivella, A.; Roubin, P.; Theulé, P.; Rajzmann, M.; Manca, C.; Coussan, S. UV and IR

Photoisomerization of Acetylacetone in a Nitrogen Matrix. *J. Phys. Chem. A*, **2007**, *111*, 3074-3081.

(9) Coe, J. D.; Ong, M. T.; Levine, G.; Martinez, T. J. On the Extent and Connectivity of Conical Intersection Seams and the Effects of Three-State Intersections. *J. Phys. Chem. A*, **2008**, *112*, 12559-12567.

(10) Upadhyaya, H. P.; Kumar, A.; Naik, P. D. Photodissociation Dynamics of Enolic-Acetylacetone at 266, 248 and 193 nm: Mechanism and Nascent State Product Distribution of OH. *J. Chem. Phys.*, **2003**, *118*, 2590-2598.

(11) Chen, X-B.; Fang, W-H.; Phillips D. L. Theoretical Studies of the Photochemical Dynamics of Acetylacetone: Isomerization, Dissociation, and Dehydration Reactions. *J. Phys. Chem. A*, **2006**, *110*, 4434-4441.

(12) Poisson, L.; Roubin, P.; Coussan, S.; Soep B.; Mestdagh, J-M. Ultrafast Dynamics of Acetylacetone (2,4-Pentanedione) in the S_2 State. *JACS*, **2008**, *130*, 2974-2983.

(13) Abdel-Shafi, A. A.; Worrall, D. R. Mechanism of the Excited Singlet and Triplet States Quenching by Molecular Oxygen in Acetonitrile. *Journal of Photochemistry and Photobiology A: Chemistry*, **2005**, *172*, 170-179.

(14) Schweitzer, C.; Mehrdad, Z.; Noll, A.; Grabner, E.-W.; Schmidt, R. Mechanism of Photosensitized Generation of Singlet Oxygen during Oxygen Quenching ofTriplet States and the General Dependence of the Rate Constants and Efficiencies of $O_2(^1\Sigma_g^+)$, $O_2(^1\Delta_g)$, and $O_2(^3\Sigma_g^-)$ Formation on Sensitizer Triplet State Energy and Oxidation Potential. *J. Phys. Chem. A*, **2003**, *107*, 2192-2198.

(15) Gijzeman, O. L. J.; Kaufman, F.; Porter, G. Oxygen Quenching of Aromatic Triplet States in Solution. *J. Chem. Soc. Faraday Trans. II*, **1973**, *69*, 708-720.

(16) Patterson, L. K.; Porter, G.; Topp, M. R.Oxygen Quenching of Singlet and Triplet States. *Chem. Phys. Lett.*, **1970**, *7*, 612-614.

(17) Lozada-Garcia, R. R.; Ceponkus, J.; Chevalier, M.; Wutharat, C.; Mestdagh J-M; Crépin, C. Nuclear Spin Conversion to Probe the Methyl Rotation Effect on Hydrogen-Bond and Vibrational Dynamics. *Angewandte Chimie International Edition*, **2012**, *51*, 6947-6950.

(18) Coussan, S.; Bouteiller, Y.; Perchard, J.; Brenner, V.; Millié, P.; Zheng, W.; Talbot, F. Methanol-acetonitrile Complexes Trapped in Argon and Nitrogen Matrices: Infrared Induced Isomerization and Theoretical Calculations . *J. Chem. Phys.*, **1999**, *110*, 10046-10057.

(19) Coussan, S.; Brenner, V.; Perchard, J.; Zheng, W. Methanol-pyridine Complexes Trapped in Argon and Nitrogen Matrices: Infrared Induced Isomerization and Theoretical Calculations. *J. Chem. Phys.*, **2000**, *113*, 8059-8069.

(20) Coe, J. D.; Martinez, T. J. Ab Initio Molecular Dynamics of Excited-State Intramolecular Proton Transfer around a Three-State Conical Intersection in Malonaldehyde. *J. Phys. Chem. A*, **2006**, *110*, 618-630.

(21) Yoon, M. C.; Choi, Y. S.; Kim S. K. Photodissociation Dynamics of Acetylacetone: The OH Product State Distribution. *J. Chem. Phys.*, **1999**, *110*, 11850-11855.

(22) Choi, C.; Pintar, M. Tunneling Splitting Due to Weak Coupling between Methyl Rotators in Acetylacetone. *J. Chem. Phys.*, **1997**, *106*, 3473-3476.